Validation of Skeletal Muscle Models in Multibody Dynamics

Sérgio B. Gonçalves[1*], Mariana Rodrigues da Silva[2,3*], Filipe Marques[2,3], Paulo Flores[3]
Miguel Tavares da Silva[1]

[1]*IDMEC, Instituto Superior Técnico, Universidade de Lisboa, Lisboa, Portugal*
{sergio.goncalves, MiguelSilva}@tecnico.ulisboa.pt

[2]*CMEMS-UMinho, Department of Mechanical Engineering, University of Minho, Guimarães, Portugal*
pflores@dem.uminho.pt

[3]*LABBELS – Associate Laboratory, Braga/Guimarães, Portugal*

The present benchmark problem provides a structured framework for validating musculoskeletal models developed using a multibody dynamics formulation. Relying on simplified biomechanical representations, five benchmark cases are proposed to progressively guide the implementation and validation of muscle contraction dynamics and musculotendon (MTU) models. This approach was chosen to introduce straightforward theoretical scenarios that are easy to interpret and serve as foundational examples for developing and validating muscle models. Specifically, the first case focuses on validating the muscle contraction dynamics model. The second case introduces MTUs with via-points. The third addresses the muscle force-sharing problem. The fourth and fifth cases evaluate the model's ability to predict the neutralizing actions of antagonist muscles and to handle biarticular muscle modeling, respectively. This submission compiles and expands upon the results presented in:

- [1] S.B. Gonçalves, M.R. da Silva, F. Marques, P. Flores, M.T. da Silva, *Validation of Skeletal Muscle Models in Multibody Dynamics: A Collaborative Collection of Benchmark Cases*, Multibody Syst Dyn (2025). https://doi.org/10.1007/s11044-025-10096-8.

In this benchmark problem, skeletal muscles are modeled using a Hill-type muscle model with a rigid tendon. Geometrically, each musculotendon unit MTU is defined by the coordinates of a series of points connected by line segments. To analyze the proposed cases, a Newton–Euler formulation is employed using two types of global coordinates: the Cartesian coordinates [2] and the fully Cartesian coordinates with a generic rigid body (FCC-GRB) [3–5]. All five problems are solved from an inverse dynamics perspective using static optimization.

The procedure for implementing the muscle contraction dynamics model and integrating it within a multibody framework is described in [1]. In this work, a detailed description of the biomechanical models, initial conditions, and motion drivers used in the five benchmark cases is provided, along with a comprehensive presentation of the results. For additional information, the reader is referred to the cited references and the current document.

*These two authors contributed equally to this work and shared co-first authorship

1. Implementation of the Benchmark Cases

A summary of the implementation steps required to integrate MTUs within a multibody framework and to validate them using the proposed benchmark cases is presented in Fig. 1.

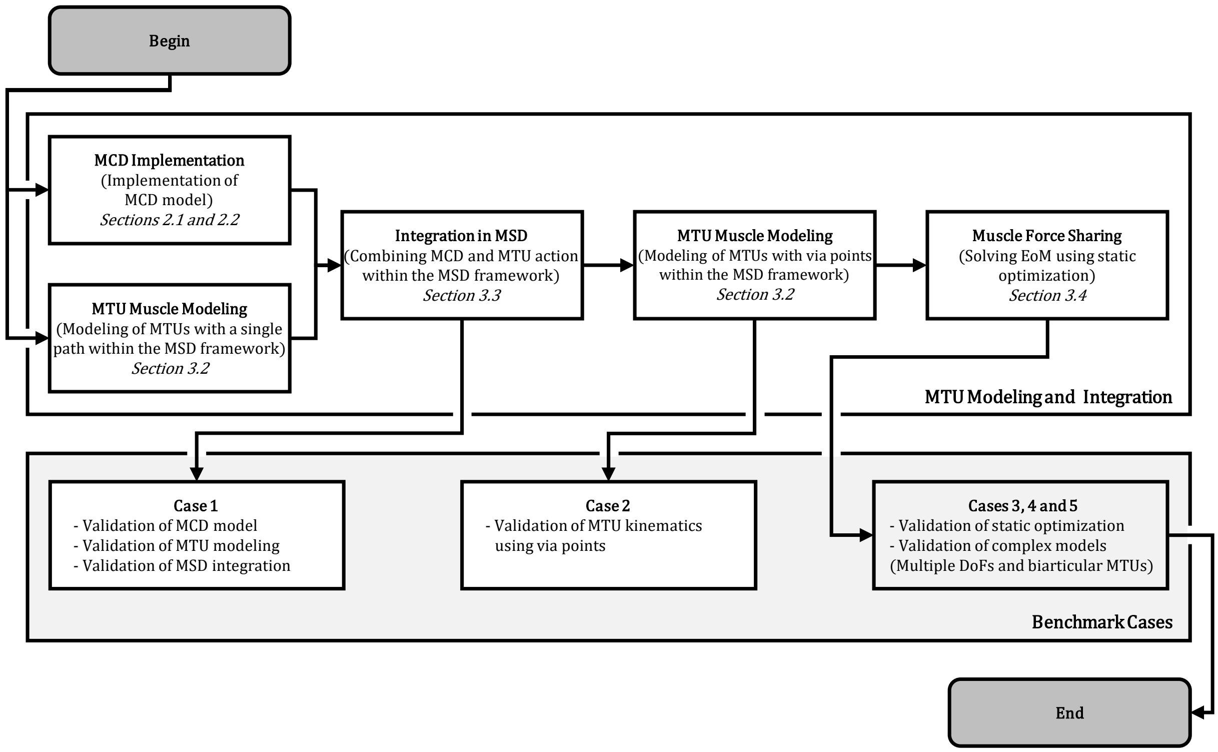

Fig. 1 – Flowchart representing the steps required to integrate and validate MTUs within a multibody framework considering the proposed benchmark cases. (Note: refer to [1] for a detailed description of the integration procedure)

In cases 1 to 4, the biomechanical model consists of two articulated rigid bodies. These bodies, referred to as body 1 and body 2, are modeled as solid cylinders with a radius of 0.025 m. The two bodies are kinematically connected by either a single revolute joint (used in cases 1, 2, and 3), which permits motion in the sagittal plane (*xz*-plane) around the *y*-axis, or a classical universal joint (used in case 4), which constrains the longitudinal rotation of body 2. Case 5 builds upon case 3 by introducing a third rigid body (body 3), which is connected to body 2 via a revolute joint, resulting in a triple-pendulum multibody model. Body 3 is also modeled as a solid cylinder with a radius of 0.025 m. The local reference frame of each body is located at its center of mass (CoM) and aligned with its principal axes of inertia (see Fig. 2). The dimensions and inertial properties of each body, along with the local coordinates of the joints, are provided in Table 1 and Table 2.

Table 1 – Dimensions and inertial properties of the rigid bodies composing the multibody models

Body (nr.)	Length [m]	Mass [kg]	Moment of inertia [kg·m^2]		
			$I_{\xi\xi}$	$I_{\eta\eta}$	$I_{\zeta\zeta}$
Body 1 (1)	1.0000	1. 0000	0.083(3)	0.083(3)	3.125×10^{-4}
Body 2 (2)	1. 0000	1. 0000	0.083(3)	0.083(3)	3.125×10^{-4}
Body 3 (3)	1. 0000	1. 0000	0.083(3)	0.083(3)	3.125×10^{-4}

Table 2 – Local coordinates and local reference frame relations of the joints composing the multibody models

Joint	Benchmark Cases	Type	Body (nr.)	Joint local coordinates ξ_{J_k}[m]	η_{J_k}[m]	ζ_{J_k}[m]	LRF relations
J_0	1-5	Fixed	1	0.0000	0.0000	0.5000	
J_1	1,2,3,5	Revolute	1	0.0000	0.0000	-0.5000	$\boldsymbol{\eta}_1 \parallel \boldsymbol{\eta}_2$
			2	0.0000	0.0000	0.5000	
J_1	4	Universal	1	0.0000	0.0000	-0.5000	$\boldsymbol{\eta}_1 \parallel \boldsymbol{\eta}_2$
			2	0.0000	0.0000	0.5000	
J_2	5	Revolute	2	0.0000	0.0000	-0.5000	$\boldsymbol{\xi}_2 \perp \boldsymbol{\eta}_3$
			3	0.0000	0.0000	0.2500	

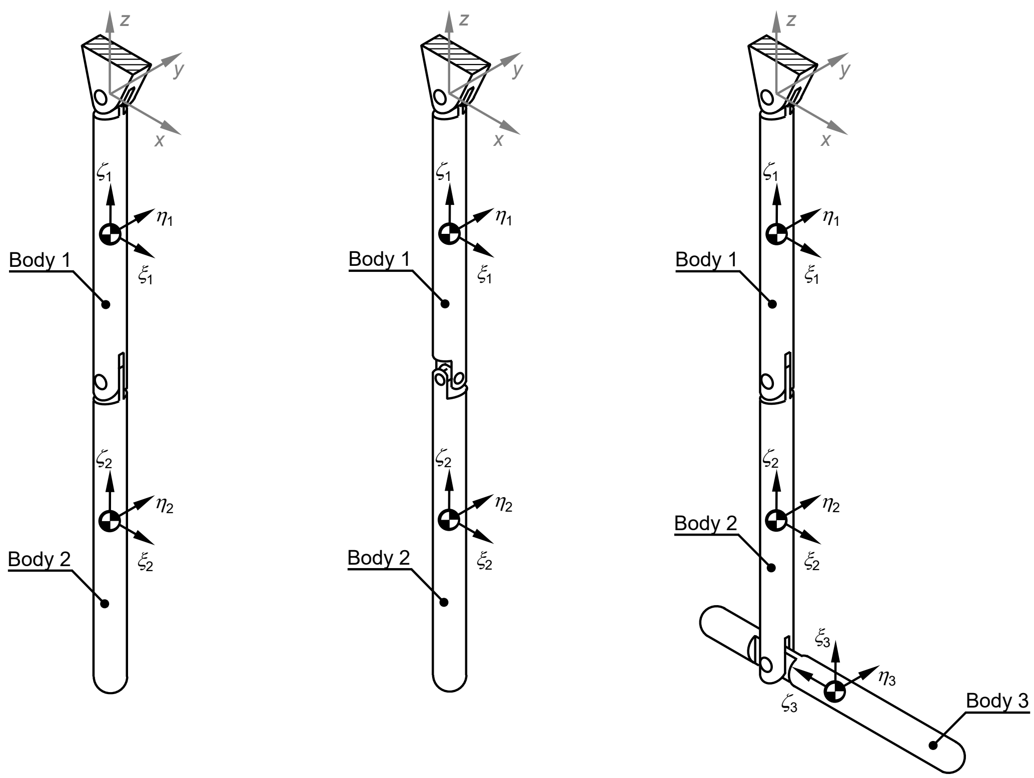

(a) (b) (c)

Fig. 2 – Schematic representation of the multibody models considered for the benchmark: (a) cases 1-3; (b) case 4; (c) case 5 utilized for case 5.

In all cases, the translation and orientation of body 1 are constrained by a fixed joint located at its center of mass (CoM). The models used in cases 1 to 3 have a single rotational degree of freedom (DoF), whereas those in cases 4 and 5 allow two rotational DoFs. The initial configuration of the biomechanical models is shown in Fig. 2, and the corresponding initial conditions are listed in Table 3 and Table 4.

Table 3 – Initial conditions for cases 1 to 4 considering an MSD formulation with Cartesian coordinates and FCC-GRB

Both Formulations							
Body (nr.)	x [m]	y [m]	z [m]		v_x [m.s^{-1}]	v_y [m.s^{-1}]	v_z [m.s^{-1}]
Body 1 (1)	0.0000	0.0000	-0.5000		0.0000	0.0000	0.0000
Body 2 (2)	0.0000	0.0000	-1.5000		0.8224	0.0000	0.0000

Cartesian Coordinates							
Body (nr.)	e_0 [ ]	e_1 [ ]	e_2 [ ]	e_3 [ ]	ω_x [rad.s^{-1}]	ω_y [rad.s^{-1}]	ω_z [rad.s^{-1}]
Body 1 (1)	1.0000	0.0000	0.0000	0.0000	0.0000	0.0000	0.0000
Body 2 (2)	1.0000	0.0000	0.0000	0.0000	0.0000	-1.6447	0.0000

FCC-GRB							
Body (nr.)	$\mathbf{u}$ [m]	$\mathbf{v}$ [m]	$\mathbf{w}$ [m]		$\dot{\mathbf{u}}$ [m.s^{-1}]	$\dot{\mathbf{v}}$ [m.s^{-1}]	$\dot{\mathbf{w}}$ [m.s^{-1}]
Body 1 (1)	$\begin{Bmatrix} 1.0000 \\ 0.0000 \\ 0.0000 \end{Bmatrix}$	$\begin{Bmatrix} 0.0000 \\ 1.0000 \\ 0.0000 \end{Bmatrix}$	$\begin{Bmatrix} 0.0000 \\ 0.0000 \\ 1.0000 \end{Bmatrix}$		$\begin{Bmatrix} 0.0000 \\ 0.0000 \\ 0.0000 \end{Bmatrix}$	$\begin{Bmatrix} 0.0000 \\ 0.0000 \\ 0.0000 \end{Bmatrix}$	$\begin{Bmatrix} 0.0000 \\ 0.0000 \\ 0.0000 \end{Bmatrix}$
Body 2 (2)	$\begin{Bmatrix} 1.0000 \\ 0.0000 \\ 0.0000 \end{Bmatrix}$	$\begin{Bmatrix} 0.0000 \\ 1.0000 \\ 0.0000 \end{Bmatrix}$	$\begin{Bmatrix} 0.0000 \\ 0.0000 \\ 1.0000 \end{Bmatrix}$		$\begin{Bmatrix} 0.0000 \\ 0.0000 \\ 1.6447 \end{Bmatrix}$	$\begin{Bmatrix} 0.0000 \\ 0.0000 \\ 0.0000 \end{Bmatrix}$	$\begin{Bmatrix} -1.6447 \\ 0.0000 \\ 0.0000 \end{Bmatrix}$

Table 4 – Initial conditions for case 5 considering an MSD formulation with Cartesian coordinates and FCC-GRB

Both Formulations							
Body (nr.)	x [m]	y [m]	z [m]		v_x [m/s]	v_y [m/s]	v_z [m/s]
Body 1 (1)	0.0000	0.0000	-0.5000		0.0000	0.0000	0.0000
Body 2 (2)	0.0000	0.0000	-1.5000		-0.4112	0.0000	0.0000
Body 3 (3)	0.2500	0.0000	-2.0000		-0.8224	0.0000	-0.2056

Cartesian Coordinates							
Body (nr.)	e_0 [ ]	e_1 [ ]	e_2 [ ]	e_3 [ ]	ω_x [rad.s^{-1}]	ω_y [rad.s^{-1}]	ω_z [rad.s^{-1}]
Body 1 (1)	1.0000	0.0000	0.0000	0.0000	0.0000	0.0000	0.0000
Body 2 (2)	1.0000	0.0000	0.0000	0.0000	0.0000	0.8224	0.0000
Body 3 (3)	0.7071	0.0000	-0.7071	0.0000	0.0000	0.8224	0.0000

FCC-GRB						
Body (nr.)	$\mathbf{u}$ [m]	$\mathbf{v}$ [m]	$\mathbf{w}$ [m]	$\dot{\mathbf{u}}$ [m.s^{-1}]	$\dot{\mathbf{v}}$ [m.s^{-1}]	$\dot{\mathbf{w}}$ [m.s^{-1}]
Body 1 (1)	$\begin{Bmatrix} 1.0000 \\ 0.0000 \\ 0.0000 \end{Bmatrix}$	$\begin{Bmatrix} 0.0000 \\ 1.0000 \\ 0.0000 \end{Bmatrix}$	$\begin{Bmatrix} 0.0000 \\ 0.0000 \\ 1.0000 \end{Bmatrix}$	$\begin{Bmatrix} 0.0000 \\ 0.0000 \\ 0.0000 \end{Bmatrix}$	$\begin{Bmatrix} 0.0000 \\ 0.0000 \\ 0.0000 \end{Bmatrix}$	$\begin{Bmatrix} 0.0000 \\ 0.0000 \\ 0.0000 \end{Bmatrix}$
Body 2 (2)	$\begin{Bmatrix} 1.0000 \\ 0.0000 \\ 0.0000 \end{Bmatrix}$	$\begin{Bmatrix} 0.0000 \\ 1.0000 \\ 0.0000 \end{Bmatrix}$	$\begin{Bmatrix} 0.0000 \\ 0.0000 \\ 1.0000 \end{Bmatrix}$	$\begin{Bmatrix} 0.0000 \\ 0.0000 \\ -0.8224 \end{Bmatrix}$	$\begin{Bmatrix} 0.0000 \\ 0.0000 \\ 0.0000 \end{Bmatrix}$	$\begin{Bmatrix} 0.8224 \\ 0.0000 \\ 0.0000 \end{Bmatrix}$
Body 3 (3)	$\begin{Bmatrix} 0.0000 \\ 0.0000 \\ 1.0000 \end{Bmatrix}$	$\begin{Bmatrix} 0.0000 \\ 1.0000 \\ 0.0000 \end{Bmatrix}$	$\begin{Bmatrix} -1.0000 \\ 0.0000 \\ 0.0000 \end{Bmatrix}$	$\begin{Bmatrix} 0.8224 \\ 0.0000 \\ 0.0000 \end{Bmatrix}$	$\begin{Bmatrix} 0.0000 \\ 0.0000 \\ 0.0000 \end{Bmatrix}$	$\begin{Bmatrix} 0.0000 \\ 0.0000 \\ 0.8224 \end{Bmatrix}$

To solve the muscle redundancy problem, the optimization scheme described in Section 3.4 of [1] was employed, using the *fmincon* solver from MATLAB's Optimization Toolbox™. At each time step, the initial guess was set to the solution from the previous frame. For the first time step, muscle activations were initialized to 0.5, $\boldsymbol{\lambda}^*$ was set to 0, and the remaining Lagrange multipliers to 1. The default optimization parameters were used (Constraint tolerance: 10^{-6}; Optimality tolerance: 10^{-6}) and the bounds for the $\boldsymbol{\lambda}^*$ were set to 10^{-15}. Gradients of both the objective function and the equality constraints were provided to the solver. For all benchmark cases, the simulation time was set to 2.00 s. Gravitational acceleration was defined to act in the negative *z*-direction with a magnitude of 9.81 m.s^{-2}.

Computational performance and accuracy were evaluated by analyzing the magnitude of constraint violations in the kinematic analysis, as well as key optimization metrics, including the number of iterations, number of function evaluations, and final constraint violations. Additionally, the computational time required for the optimization process was recorded.

Fig. 3 provides a schematic representation of the five benchmark cases proposed in this work. It is important to note that MTUs located on the positive side of the x-axis are designated as flexors, whereas those on the negative side are classified as extensors. All MTUs were defined using similar properties: (*i*) the optimal muscle fiber length (l_0^M) and the tendon slack length (l_S^T) are defined to represent 1/4 and 3/4 of the reference MTU length defined for each problem (l_{ref}^{MT}), respectively, (*ii*) the pennation angle at the optimal fiber length (α_0^M) is set to 10º, and (*iii*) the maximum contraction velocity ($\dot{l}_0^M$) is defined as 1/10 of l_0^M. The value of l_0^{MT} for each muscle is defined such that the normalized muscle length (l^M/l_0^M) remains close to 1 throughout the entire analysis. Detailed parameters for each muscle, including the location of the MTU origin, insertion, and via-points, as well as the peak isometric active force, are provided in Table 5.

Table 5 – Parameters utilized for the MTUs considered in the multibody models of each benchmark case

	MTU name	f_0^M [m]	l_{ref}^{MT} [m]	Body name	Point name	Local coordinates of the points [m] ξ	η	ζ
Benchmark Case 1	Flexor (F)	100	1.100	Body 1	Origin	0.075	0.000	0.500
				Body 2	Insertion	0.075	0.000	0.400
	Extensor (E)	100	1.050	Body 1	Origin	-0.100	0.000	0.500
				Body 2	Insertion	-0.100	0.000	0.450
Benchmark Case 2	Flexor (F)	100	1.100	Body 1	Origin	0.075	0.000	0.500
				Body 1	Via-point	0.075	0.000	-0.500
				Body 2	Insertion	0.025	0.000	0.400
	Extensor (E)	100	1.050	Body 1	Origin	-0.100	0.000	0.500
				Body 1	Via-point	-0.100	0.000	-0.450
				Body 2	Insertion	-0.050	0.000	0.450
Benchmark Cases 3 and 4	Medial Flexor (F_{Med})	100	1.150	Body 1	Origin	0.075	0.100	0.500
				Body 1	Via-point	0.075	0.100	-0.500
				Body 2	Insertion	0.050	0.025	0.400
	Medial Extensor (E_{Med})	25	1.100	Body 1	Origin	-0.100	0.100	0.500
				Body 1	Via-point	-0.100	0.100	-0.450
				Body 2	Insertion	-0.050	0.025	0.450
	Lateral Flexor (F_{Lat})	50	1.100	Body 1	Origin	0.075	-0.050	0.500
				Body 1	Via-point	0.075	-0.050	-0.500
				Body 2	Insertion	0.050	-0.025	0.400
	Lateral Extensor (E_{Lat})	50	1.100	Body 1	Origin	-0.100	-0.050	0.500
				Body 1	Via-point	-0.100	-0.050	-0.450
				Body 2	Insertion	-0.050	-0.025	0.450
Benchmark Case 5	Joint 1 Flexor (F_1)	100	1.100	Body 1	Origin	0.075	0.000	0.500
				Body 1	Via-point	0.075	0.000	-0.500
				Body 2	Insertion	0.025	0.000	0.400
	Joint 1 Extensor (E_1)	100	1.050	Body 1	Origin	-0.100	0.000	0.500
				Body 1	Via-point	-0.100	0.000	-0.450
				Body 2	Insertion	-0.050	0.000	0.450
	Joint 2 Flexor (F_2)	100	0.900	Body 2	Origin	0.075	0.000	0.400
				Body 2	Via-point	0.075	0.000	-0.400
				Body 3	Insertion	0.050	0.000	0.100
	Joint 2 Extensor (E_2)	100	0.900	Body 2	Origin	-0.100	0.000	0.400
				Body 2	Via-point	-0.100	0.000	-0.400
				Body 3	Insertion	0.025	0.000	0.400
	Joint 1 and 2 Extensor ($E_{1,2}$)	100	1.075	Body 1	Origin	-0.150	0.000	-0.400
				Body 2	Via-point	-0.150	0.000	0.400
				Body 2	Via-point	-0.100	0.000	-0.400
				Body 3	Insertion	0.025	0.000	0.400

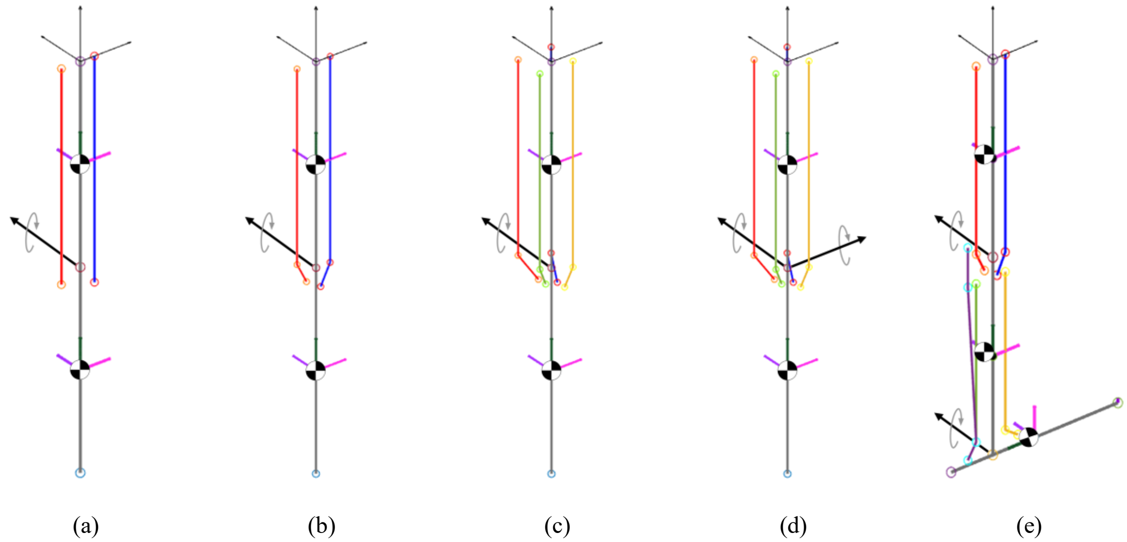

Fig. 3 – Schematic representation of the biomechanical models considered in the benchmark problems: a) Case 1 – MCD without via-points, b) Case 2 – MCD with one via-point, c) Case 3 – muscle redundancy, d) Case 4 – muscle neutralizing action, e) Case 5 – biarticular muscle modeling.

1.1. Case 1 – Muscle Contraction Dynamics

Case 1 consists of two rigid bodies connected by a revolute joint, allowing motion exclusively in the sagittal plane (*xz*-plane). The proximal end of body 1 is fixed to the ground at the origin of the global reference frame via a fixed joint. A pair of antagonistic muscles is modeled, each defined by two points corresponding to the origin and insertion of the MTUs (see Table 5). The DoF associated with the revolute joint is guided by an angular driving constraint, defined by a sinusoidal function with an amplitude of 30° and a period of 2 seconds, oscillating around the initial position (see Fig. 4). A schematic representation of the movement, showcasing the position of the system in five different time frames, is presented in Fig. 5.

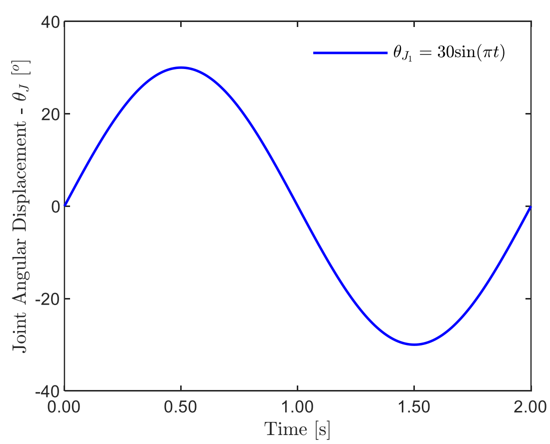

Fig. 4 – Rotational driver applied to guide the angular DoF of the revolute joint between bodies 1 and 2 (θ_{J_i}) in cases 1 to 4.

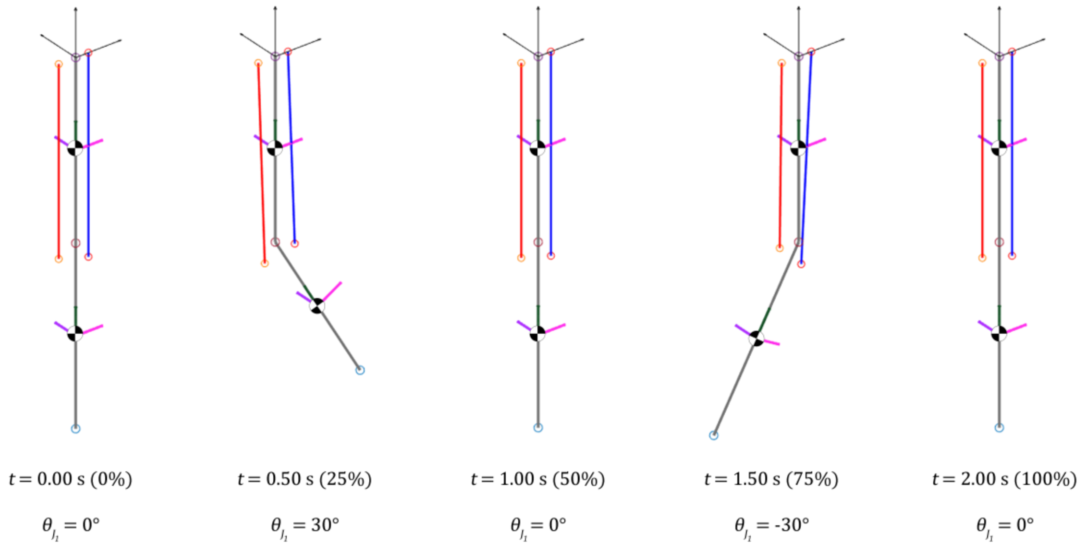

Fig. 5 – Snapshots of the movement of the biomechanical model utilized in benchmark case 1 for the 2.00-second simulation.

The main goal of this benchmark case is to validate the MCD model by providing reference data for verifying the correct computation of all relevant parameters. Specifically, this case analyzes the evolution of MTU and muscle kinematics, including MTU length, muscle length, muscle contraction velocity, and pennation angle, throughout the motion cycle. Additionally, Case 1 evaluates the force generated by various muscle components, such as the total MTU force, passive force, and contractile force, along with the parameters required for their computation: the force–length relationship, the force–velocity relationship, and the maximum contractile force the muscle can produce in its current state.

1.2. Case 2 – Muscle Kinematics with Via Points

In this second case, the same biomechanical model and the two MTUs from the first case are used. The angular driving constraint shown in Fig. 4 is also applied to control the motion of the revolute joint. However, in the present case, a via-point is introduced in each MTU to better define the muscle path (see Table 5 and Fig. 3b). The objective of this case is to validate the modeling of MTUs that include via-points and to assess their impact on the calculation of muscle parameters, specifically muscle fiber length, the force–length and force–velocity relationships, and the maximum force the muscle can produce.

1.3. Case 3 – Muscle Force Sharing Problem

The multibody model used in Case 3 is identical to that of Case 2, and the angular driving constraint shown in Fig. 4 is again used to control the motion of the revolute joint. However, instead of using two MTUs aligned with the rigid bodies in the sagittal plane, Case 3 includes four MTUs distributed across the four quadrants of the bodies in the transverse plane, as schematically illustrated in Fig. 3c. Two of these MTUs are positioned anteriorly relative to the bodies, one medially and the other laterally and are responsible for controlling flexion (F_{Med} and F_{Lat}). Similarly, the other MTU pair is positioned posteriorly, controlling the extension (E_{Med} and E_{Lat}).

The inclusion of two muscle pairs to control flexion and extension of body 2 introduces muscle redundancy, meaning that multiple activation patterns can achieve the same prescribed motion. The main objective of Case 3 is to evaluate whether the optimization-based analysis can successfully address this redundancy. It is expected that the solution will converge to an activation pattern that distributes effort between the two muscles in each pair, thereby minimizing overall muscle stress.

1.4. Case 4 – Muscle Neutralizing Action

The fourth benchmark case is similar to Case 3, however, the revolute joint connecting the two bodies is replaced with a classical universal joint, which provides two rotational DoFs in the frontal and sagittal planes (see Fig. 3d). The motion of the joint in the sagittal plane (*xz*-plane) is guided using the driving constraint of Fig. 4, while the motion of the joint in the frontal plane (*yz*-plane) is held constant throughout the analysis using a driving constraint that ensures a parallel relation between the basis vectors $\boldsymbol{\eta}$ of bodies 1 and 2.

This modification implies that the flexor (F_{Med} and F_{Lat}) and extensor muscles (E_{Med} and E_{Lat}), which are not strictly aligned with the sagittal plane, also generate moments in the horizontal plane. Therefore, the primary objective of Case 4 is to assess whether the simulation converges to an optimal solution that minimizes muscle activations required to produce the prescribed motion in the sagittal plane, while simultaneously reducing net moments in the frontal plane. Additionally, the case aims to evaluate the neutralizing action of antagonist muscles at specific time points, where they counteract the abduction moments generated by agonist muscles, thereby reducing overall muscle stress.

1.5. Case 5 – Biarticular Muscle Action

The fifth benchmark case consists of three rigid bodies connected by two revolute joints (between bodies 1 and 2, and between bodies 2 and 3) (see Fig. 3e). The translation and orientation of body 1 are constrained by the use of a fixed joint. The inertial properties of the three bodies can be consulted in Table 2.

For simplicity, the joint connecting bodies 1 and 2 is hereafter termed J_1, while the joint between bodies 2 and 3 is termed J_2. The two MTUs employed for actuating the J_1 in case 2 (F_1 and E_1) are also utilized in case 5 for the same purpose. However, one additional pair of uniarticular muscles is introduced in case 5, that is, one for extension (E_2) and another for flexion (F_2) of J_2. Additionally, a biarticular muscle ($E_{1,2}$) is included in the multibody model to simultaneously allow extension of J_1 and J_2. The anthropometric properties of the muscles, as well as the location of the origin, insertion, and via points are detailed in Table 5.

Joint J_1 is actuated using a half-sinusoidal angular driver with an amplitude of 30° and a period of 4 seconds (see Fig.6). This motion represents the movement of J_1 from the neutral position to a 30° extension, followed by a return to the initial position. In turn, a constant angle driver was applied to joint J_2, maintaining the angle between bodies 2 and 3 at 90º throughout the simulation. To force the activation of the extensor muscles associated with J_2, a concentrated external force with a constant magnitude of 20 N, oriented in the positive global *z*-direction, is applied at the most distal point of body 3 (see Fig. 7). Fig. 7 shows several snapshots of the movement of the multibody model guided with the driving constraint presented in Fig.6, during the 2.00-second simulation.

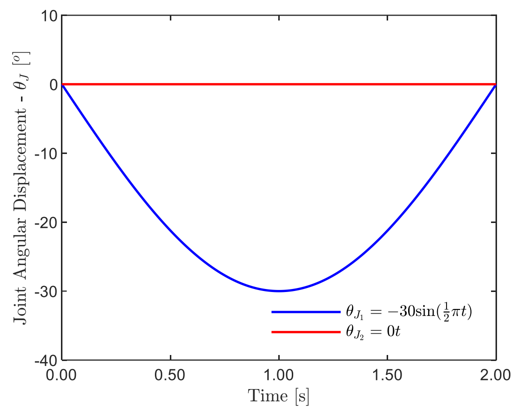

Fig.6 – Rotational drivers applied to guide the angular DoFs of the revolute joints between bodies 1 and 2 (θ_{J_1}) and between bodies 2 and 3 (θ_{J_1}) in case 5.

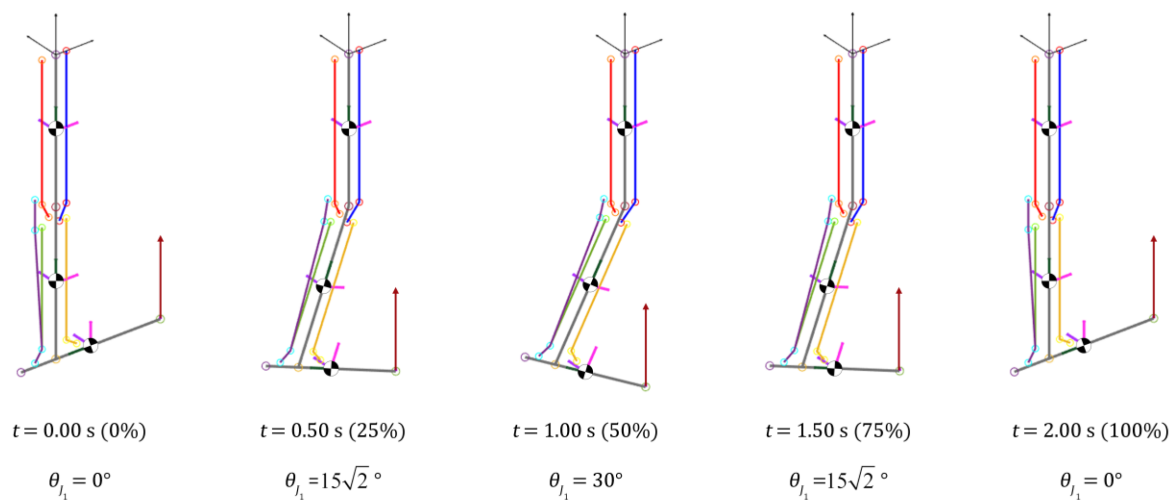

Fig. 7 – Snapshots of the movement of the biomechanical model utilized in benchmark case 5 for the 2-second simulation (Note: The wine-colored vector represents the external force applied in the tip of body 3).

The objective of this benchmark case is to evaluate whether the optimizer converges to a solution that prioritizes the activation of the biarticular muscle over the combined action of the two uniarticular muscles. To this end, a scenario is considered in which the desired movement requires simultaneous extension at both joints: controlling the flexion of joint J_1 and counteracting the external force applied at the distal end of body 3 in order to maintain joint J_2 in a neutral position. Since the biarticular muscle can perform the extension of both joints simultaneously, it is anticipated that the optimizer will favor its activation to minimize the overall muscle stress, rather than relying on the combined action of the two uniarticular muscles, which would achieve the same movement with potentially greater stress.

2. Data Report

The results are presented at a sampling frequency of 100 Hz, with each file beginning with a header to facilitate the interpretation of the columns. For each MTU considered in the problem, the data is organized in the following order: 1) Time – t [s]; 2) Muscle activation – a^M [ ]; 3) MTU force – $\mathbf{f}^{MT}$

[N]; 4) CE force – $\mathbf{f}_{CE}^{M}$ [N]; 5) PE force – $\mathbf{f}_{PE}^{M}$ [N]; 6) maximum contractile force for the current state – $\hat{f}_{CE}^{M}$ [N]; 7) MTU length – l^{MT} [m]; 8) Normalized muscle fiber length – l^{M}/l_{0}^{M} [ ]; 9) Muscle pennation angle – α^{M} [rad]; 10) Force-length relationship – f_{l}^{M} [ ]; and 11) Force-velocity relationship – f_{v}^{M} [ ]. Additionally, six columns are included at the end of the results matrix to describe the position and velocity of the CoM for each body in the system. A supplementary PDF file was also added, providing details on the optimization performance and accuracy metrics, including computation time, number of iterations, number of function evaluations, and violation of the optimization final constraints. An example of the results of the benchmark problems is presented in Fig. 8

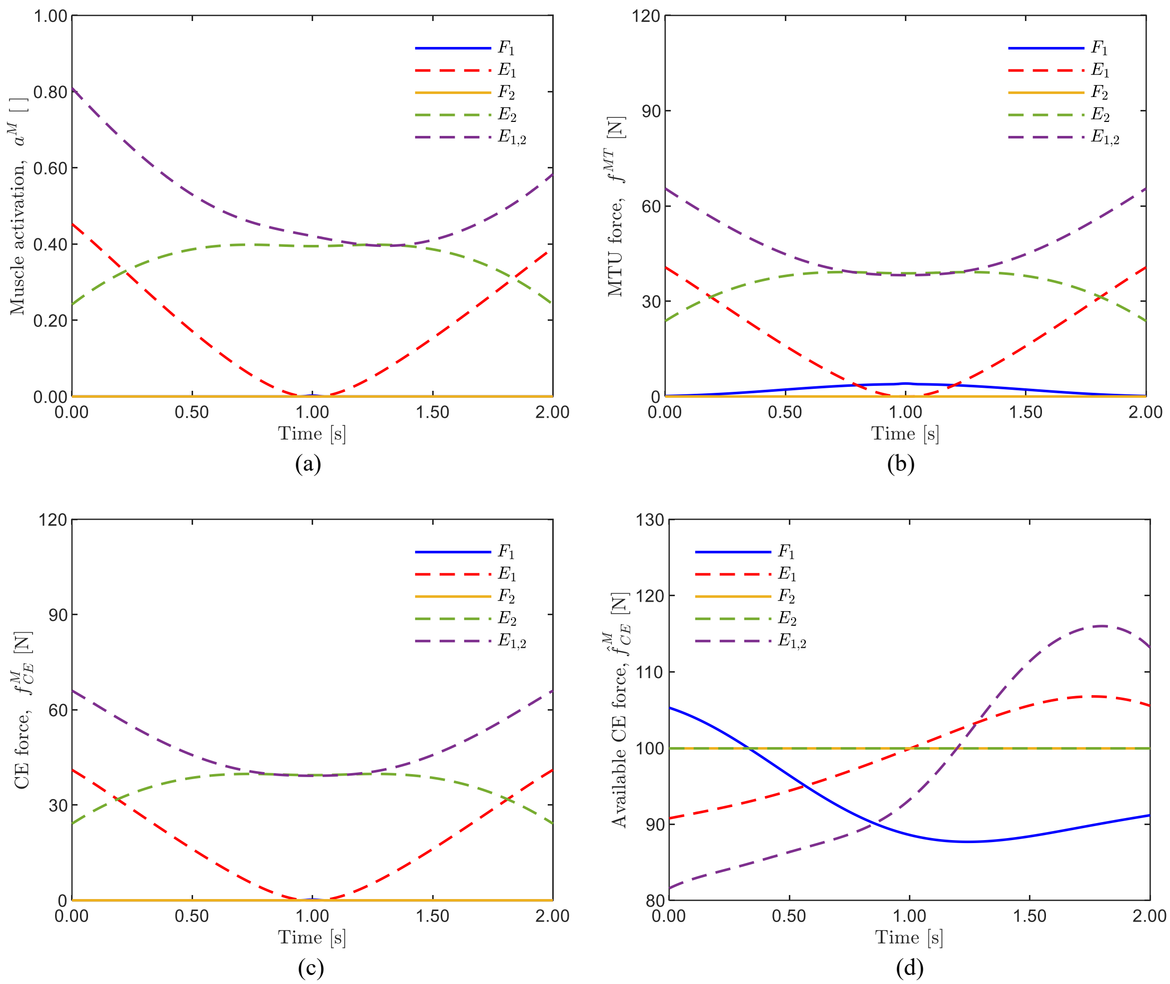

Fig. 8 – (a) Muscle activation (b) MTU force, (c) CE force and (d) PE force for the benchmark case 5 (Note: F_1 – Joint 1 flexor MTU; E_1 – Joint 1 extensor MTU; F_2 – Joint 2 flexor MTU; E_2 – Joint 2 extensor MTU; $E_{1,2}$ – Joints 1 and 2 extensor MTU).

3. Remarks

It should be noted that, although similar expressions are available in the literature for describing the force–length and force–velocity relationships, differences exist between them (e.g., [6–10]). Likewise, the values for muscle-specific tension vary across different sources (e.g., [11–13]). These discrepancies may influence the calculation of the maximum contractile force for the current state, as well as the value of the objective function, thereby leading to different activation values. Therefore, when implementing the proposed benchmark cases in other existing platforms, special care must be taken to ensure that the same force-length and force-velocity formulations are used, and that the objective function is adapted to match the one presented in [1]. This alignment is essential for enabling direct and meaningful comparisons.

References

[1] S.B. Gonçalves, M.R. da Silva, F. Marques, P. Flores, M.T. da Silva, Validation of Skeletal Muscle Models in Multibody Dynamics: A Collaborative Collection of Benchmark Cases, Multibody Syst Dyn (2025). https://doi.org/10.1007/s11044-025-10096-8.

[2] P. Nikravesh, Computer-aided analysis of mechanical systems, Prentice-Hall, Inc., 1988.

[3] I. Roupa, S.B. Gonçalves, M.T. Silva, Kinematics and dynamics of planar multibody systems with fully Cartesian coordinates and a generic rigid body, Mech Mach Theory 180 (2023) 105134. https://doi.org/10.1016/j.mechmachtheory.2022.105134.

[4] S.B. Gonçalves, I. Roupa, P. Flores, M. Tavares da Silva, Kinematic and Dynamic Analysis of Spatial Multibody Systems with Fully Cartesian Coordinates and a Generic Rigid Body, Mech Mach Theory 209 (2025) 1–35. https://doi.org/10.1016/j.mechmachtheory.2025.105955.

[5] S.B. Gonçalves, I. Roupa, M. Tavares da Silva, On the Analysis of Fully Cartesian Coordinates – A Comparison between a Reduced and Full-Defined Modelling Approach in Spatial Mechanisms, in: ECCOMAS Thematic Conference on Multibody Dynamics 2023, Lisbon, Portugal, 2023.

[6] M.T. Silva, Human motion analysis using multibody dynamics and optimization tools., PhD thesis in Mechanical Engineering. Universidade Técnica de Lisboa, Instituto Superior Técnico, 2003.

[7] T.S. Buchanan, D.G. Lloyd, K. Manal, T.F. Besier, Estimation of muscle forces and joint moments using a forward-inverse dynamics model, Med Sci Sports Exerc 37 (2005) 1911–1916.

[8] F. Romero, F.J. Alonso, A comparison among different Hill-type contraction dynamics formulations for muscle force estimation, Mechanical Sciences 7 (2016) 19–29. https://doi.org/10.5194/ms-7-19-2016.

[9] D.G. Thelen, Adjustment of Muscle Mechanics Model Parameters to Simulate Dynamic Contractions in Older Adults, J Biomech Eng 125 (2003) 70–77. https://doi.org/10.1115/1.1531112.

[10] J.A.C. Martins, E.B. Pires, R. Salvado, P.B. Dinis, A numerical model of passive and active behavior of skeletal muscles, Comput Methods Appl Mech Eng 151 (1998) 419–433. https://doi.org/10.1016/S0045-7825(97)00162-X.

[11] A. Rajagopal, C.L. Dembia, M.S. DeMers, D.D. Delp, J.L. Hicks, S.L. Delp, Full-body musculoskeletal model for muscle-driven simulation of human gait, IEEE Trans Biomed Eng 63 (2016) 2068–2079. https://doi.org/10.1109/TBME.2016.2586891.

[12] G.T. Yamaguchi, Dynamic Modeling of Musculoskeletal Motion: a Vectorized Approach for Biomechanical Analysis in Three Dimensions, Springer Science & Business Media, 2005.

[13] L.S. Persad, Z. Wang, P.A. Pino, B.I. Binder-Markey, K.R. Kaufman, R.L. Lieber, Specific tension of human muscle in vivo: a systematic review, J Appl Physiol 137 (2024) 945–962. https://doi.org/10.1152/JAPPLPHYSIOL.00296.2024.